Centre for Climate Change Economics and Policy

Grantham Research Institute on Climate Change and the Environment

Probabilistic regional and seasonal predictions of twenty-first century temperature and precipitation

David Stainforth

August 2010

Centre for Climate Change Economics and Policy
Working Paper No. 27

Grantham Research Institute on Climate Change and the Environment

Working Paper No. 23

The Grantham Foundation for the Protection of the Environment

E·S·R·C Economic & Social Research Council

University of Leeds

LSE The London School of Economics and Political Science

The Centre for Climate Change Economics and Policy (CCCEP) was established by the University of Leeds and the London School of Economics and Political Science in 2008 to advance public and private action on climate change through innovative, rigorous research. The Centre is funded by the UK Economic and Social Research Council and has five inter-linked research programmes:

1. Developing climate science and economics
2. Climate change governance for a new global deal
3. Adaptation to climate change and human development
4. Governments, markets and climate change mitigation
5. The Munich Re Programme - Evaluating the economics of climate risks and opportunities in the insurance sector

More information about the Centre for Climate Change Economics and Policy can be found at: http://www.cccep.ac.uk.

The Grantham Research Institute on Climate Change and the Environment was established by the London School of Economics and Political Science in 2008 to bring together international expertise on economics, finance, geography, the environment, international development and political economy to create a world-leading centre for policy-relevant research and training in climate change and the environment. The Institute is funded by the Grantham Foundation for the Protection of the Environment, and has five research programmes:

1. Use of climate science in decision-making
2. Mitigation of climate change (including the roles of carbon markets and low-carbon technologies)
3. Impacts of, and adaptation to, climate change, and its effects on development
4. Governance of climate change
5. Management of forests and ecosystems

More information about the Grantham Research Institute on Climate Change and the Environment can be found at: http://www.lse.ac.uk/grantham.

Probabilistic Regional and Seasonal Predictions of Twenty-First Century Temperature and Precipitation

David A. Stainforth[1,2]

[1] *Grantham Research Institute, London School of Economics and Political Science, Houghton Street, London. WC2A 2AE*

[2] *Oxford University Centre for the Environment, University of Oxford, South Parks Road, Oxford. OX1 3QY*

The rationale for international agreements on climate change mitigation comes from the global scope of impacts irrespective of the location of greenhouse gas (GHG) emissions. By contrast one of the motivations for national commitments to such agreements, and for national adaptation planning, is concern about national scale impacts. Climate predictions on regional scales are therefore highly sought after by policy and decision makers, yet robust, relevant predictions on these scales raise practical and philosophical challenges for climate science[1]. Existing methods underestimate uncertainty through limited exploration of model error[2,3,4] and ad hoc choices regarding the relationship between model diversity and real world probabilities[6,7]. Here a new method is presented for extracting model based probabilistic information on regional and seasonal scales, utilising the world's largest climate ensemble exploring the consequences of model uncertainty. For the first time ensemble filtering is implemented to counter problems of in-sample bias in future analyses. A probabilistic interpretation is presented of the regional scale consequences of targets to halve global GHG emissions by 2050[8,9], using a scenario with an estimated 32% probability of exceeding 2^{o}C global warming (relative to pre-industrial levels). Meeting such a target leads to the model's winter climate for

Northern Europe being between 0.5 and 5.9^{o}C warmer and -5 and 34% wetter in the 2090s. A business-as-usual scenario provides ranges of 6.8 to 14.5^{o}C and 22 to 71%. Higher precipitation increases are found for North Asia. That these ranges are large illustrates the need for adaptation strategies which minimise vulnerability rather than optimise for the future[10]. The method is potentially useful for making probabilistic statements about future seasonal mean model temperatures in many of the 22 predominantly land regions studied, as well as for model precipitation in a small number of high latitude regions.

Probabilistic climate forecasts are most robust and best constrained for global multi-year mean near-surface temperature (T_g) because (i) observational and physical constraints on T_g minimise the impact of spatial and temporal variability, (ii) temperature is the best observed climatic variable, and (iii) it can be studied with a variety of different types of models from complicated global circulation models (GCMs), which resolve some aspects of the large scale dynamics, to simple energy balance models which explicitly average over such dynamical behaviour. Even so there remains significant uncertainty in the probability distribution for the long term T_g response to GHG stabilization scenarios, partly due to the limited ability of observations of the past to constrain feedbacks relevant to the future[11]. The nearer term transient response is better constrained[12,13]. Smaller spatial and temporal scales have many more degrees of freedom, making the evaluation of probabilistic information harder. Only GCMs provide data on regional scales yet the consequences of both aleatory and epistemic uncertainty are greater at smaller scales[1] while our ability to explore such uncertainties are reduced as a consequence of these models' computational demands. Here we combine information on model uncertainty with well-studied constraints on T_g to provide probabilistic model information on regional and seasonal scales.

Model uncertainty is evaluated with almost 40,000 simulations of the first experiment of the climate*prediction*.net project[14]; still by far the largest exploration of model uncertainty in a GCM. There will be an unavoidable bias in future analyses of this ensemble. The desire to reduce uncertainty, for example, can lead to a focus on model versions which exhibit some form of extreme behaviour[15,16]. This focus is developed "in-sample", encouraging false confidence that uncertainty has been reduced. Here, to maintain the possibility of out-of-sample verification in future analyses, we apply ensemble filtering by removing half of the post quality controlled model versions (see methods) before further analysis. The remaining simulations consist of 6203 model versions[14], each with initial condition ensembles of between 1 and 10 members. The GCM is a version of HadSM3[17]; the HadAM3[18] atmospheric model coupled to a thermodynamic ocean. Each simulation involves three 15 year phases[14]: (1) calibration, to deduce the ocean heat-flux convergence field used in subsequent phases to represent the transport of heat by ocean circulations, (2) control, to quantify the model's behaviour with pre-industrial CO_2 concentrations, and (3) doubled CO_2, to explore the response to increasing CO_2 concentrations. Regional[19] temperature and precipitation, and T_g, anomalies are extracted for each simulation as the difference between the means of years eight to fifteen in phases two and three. To separate model uncertainty from internal model variability, ensemble results are presented as the mean of these anomalies across the initial condition ensemble for each model version (figures 1 and 2).

Co-variations of simulated winter and summer, temperature and precipitation with T_g for Northern Europe (NE) and North Asia (NA) are shown in figure 1. In both regions temperature and winter precipitation show a strong correlation with T_g. Summer precipitation does not. While such correlations are unsurprising, these results enable a quantification of the relationships in this model, accounting for a degree of epistemic uncertainty (parametric but not structural) in the atmospheric response. Yet it is unclear

how to evaluate the robustness of these relationships. The lack of independence between model versions[20,21,22,1] removes the relevance of traditional goodness of fit tests, and constraints on climate ensembles remain elusive[1,23,24,14]. A simple linear least squares fit is therefore applied. As a test of sensitivity it is noted that including only those versions whose absolute global mean ocean heat-flux convergence is less than 2.5 W/m^2 (red points) has little impact on the relationships. (See supplementary fig 1 for other seasons and regions).

Probabilities of changes in T_g and atmospheric CO_2 concentrations for given scenarios can be combined with these relationships to provide estimates of their implications for regional climate change within the model. The direct effect of CO_2 increases[25], quantified by the intercept, is separated from the response associated with changes in T_g, quantified by the gradient, as discussed on the global scale by Allen and Ingram, 2002[25] (see methods). The intercept is taken to be linearly related to CO_2 increase. Again lack of independence between model versions makes the results of traditional methods for evaluating uncertainty around the central estimate uninformative; the distribution of points about the regression line is a consequence of subjective choices, amongst other things, not an objective description of uncertainty. Furthermore, the societal relevance of climate predictions argues for a conservative approach to constraining even model results; overly constrained statements encourage false confidence and risk mal-adaptation. Thus, building on the “non-discountable envelope” of possibilities approach[26] to this problem, a band of uniform probability is taken about the regression line; its width defined by the maximum range of model versions about that line (figure 1 and methods). Natural variability within the model is amenable to traditional approaches and is therefore handled separately (see methods).

The model versions include both equilibrium and non-equilibrium states but one might nevertheless question whether the bands are likely to encompass behaviour

representative of a transient response such as that to be encountered in the 21st century. Figure 2 provides some justification for confidence, subject to the assumptions discussed later. It includes data from earlier in the same simulations, where this information is available, and indicates that the method does encompass the behaviour of the very early, transient, stages of the simulations for this model.

The distributions in Figure 3 are conditional probability density functions for NE and NA model winter, deduced by combining these relationships with probability density functions (PDFs) for T_g and CO_2 concentrations from Meinshausen et al., 2009[9]. The 5-95% range for change in the 8-year mean, Northern European winter precipitation (temperature) between the late 1800s[9] and the 2090s in this model is -5% to 34% (0.5 to 5.9°C) under the halved_by_2050 scenario; 22 to 71% (6.8 to 14.5°C) for the A1F1 SRES scenario. Table 1 presents the values for other seasons and for NA. Supplementary table 4 provides results for other regions.

The assumptions necessary to relate model results to reality are the most significant aspect of any modelling study. There are three key assumptions in this approach. First the method relies on predicted distributions for T_g. While this provides flexibility to apply the T_g distribution of ones choice and removes the dependence on the global climate sensitivity of any specific model, it also integrates a dependence on the assumptions of the underlying study of T_g. Second, only changes in CO_2 concentrations are included in these simulations; changes in other greenhouse gases, particularly sulphate aerosols, will substantially affect some regions. Third, the relationships themselves could be a consequence of the model structure or the exploration of uncertain parameter values, rather than reflecting real world behaviour. The lack of a stratosphere[27], dynamic ocean, dynamic ice sheets[28], carbon cycle[29], atmospheric/oceanic chemistry, and processes which require high resolution to be resolved etc., highlight the model-based nature of these conditional PDFs. This is true of

all climate predictions; none should be used quantitatively as real-world probabilities in climate change adaptation decisions. These results nevertheless provide a significant step forward in understanding the range of regional behaviour possible in current models, which is one source of guidance for such decisions. They incorporate the largest exploration of epistemic uncertainty in the simulation of regional climate to date, and are based on consistent model behaviour across an ensemble. Unlike existing methods for the analysis of perturbed physics ensembles this does not make the assumption that model diversity relates to probabilities of real world behaviour, the ad hoc nature of which has been discussed[23,6,1]. Furthermore it is orthogonal to arguments over a means for weighting models against observations to highlight those with the most relevant feedbacks for 21st century climate[24,1].

These results combine model probabilities from initial condition ensembles with probabilities for T_g and a range of possibilities described by the perturbed physics ensemble. Maintaining the philosophy behind the envelopes of possibility approach, only the 5-95% ranges are presented. The approach provides contextual information for adaptation decisions; an alternative to datasets with more limited uncertainty exploration which potentially encourage false confidence. Increasing initial condition ensemble sizes could narrow the conditional PDFs through better quantification of the model version means for those versions which provide the outer bounds of the uniform probability bands. Increasing perturbed physics ensemble sizes could broaden the conditional PDFs through wider exploration of feedback mechanisms. Robust physically understood constraints would of course reduce uncertainty. Climate change is a problem of interlinked risks; if some model regions see only the 5% temperature change this implies that others must see much greater changes to maintain consistency with the change in T_g. Despite the large uncertainties illustrated here, the regional consequences of the two scenarios show little overlap by the end of the century. Under the A1F1 scenario even the 5% values represent significant change.

Methods Summary:

Separation of forms of uncertainty: Model version response is taken as the mean across its initial condition ensemble (ICE). The nature of the distributed modelling experiment means model versions have varying size ICEs; some have only single simulations. The linear fits are not sensitive to the minimum size ICE deemed acceptable, although the spread about the fit is. Accepting smaller ICEs leads to greater mixing of internal variability and model uncertainty and consequently greater spread. Increasing the minimum size ICE better separates the two forms of uncertainty but at the cost of reducing the total number of model versions available. Here the minimum size ICE is taken as four – reducing the total number of model versions from 6203 to 1594. Using these model versions a simple linear regression was performed for each regional variable against T_g; giving an intercept (i) and gradient (g).

Construction of Conditional PDFs: PDFs of T_g and atmospheric CO_2 concentrations were provided[9] in terms of 600 equally likely 21st century timeseries for each scenario. For each timeseries the mean T_g (mT_g) and mean atmospheric CO_2 concentration (mCO_2) was calculated for the central 8 years of the relevant decade. Assuming a linear direct response to CO_2 concentrations the central estimate for the regional variable is then calculated as:

$$\text{Regional Variable Central Estimate} = i * ((mCO_2 / p2CO_2) - 1) + g * mT_g$$

where $p2CO_2$ is the atmospheric CO_2 concentrations in the second phase of the simulations.

A range of equal probability, defined by the maximum deviation from the linear fit of any model version mean, is taken about this central estimate. A single sided Gaussian distribution is added to the lower and upper end of this range. The gaussian's variance is taken as the mean variance, allowing for uncertainty in T_g, across all initial

condition ensembles included. This provides a tail of probability which accounts for internal model variability. The resulting 600 distributions are combined and normalised to produce the conditional PDFs in figure 3.

Supplementary Information accompanies this paper.

Acknowledgements: Thanks to M. Meinshausen for scenario data on T_g and CO_2 concentrations. Thanks also to Prof. L.A. Smith, Dr. N. Ranger, Dr. A. Lopez and Dr. M. New for helpful discussions and comments on earlier drafts. Thanks to the climate*prediction*.net team and participants for enabling this research.

Author contribution: D.A.S. carried out all data analysis and wrote the paper.

Correspondence and requests for materials should be addressed to d.a.stainforth@lse.ac.uk

Figure 1: Changes in Northern European (top) and North Asian (bottom) temperature (left) and precipitation (right) with T_g, as simulated by model versions of the grand ensemble. DJF indicates winter (December/January/February), JJA summer (June/July/August). Model versions with absolute values of global mean atmosphere/ocean heat flux (H_g) less than 2.5 W/m^2 are shown in red. All points are ensemble means across initial condition ensembles where available. Crosses have at least 4 member initial condition ensembles, dots have fewer members and are omitted from further analysis – see methods. The least squared linear fits are based on crosses only; black (all model versions) and red (model versions with $|H_g| < 2.5$ W/m^2). The correlation coefficient is shown in the top left hand corner of each plot; this information is indicative only of potential relevance. The shaded band is taken as having uniform probability.

Figure 2: Black crosses are the same as in figure 1 but for temperature only: Northern Europe – left, North Asia - right. Coloured crosses are from earlier in a subset of the same simulations (only some simulations provided the necessary data). Blue crosses are calculated as the difference between the means of years one to eight from phases two and three. Orange crosses use years three to ten.

Figure 3: Conditional probability density functions for Northern European (left), and North Asian (right) winter temperature (top) and precipitation (bottom) changes. Changes in the eight year model mean are presented for the 2050s and the 2090s based on predictions of T_g and CO_2 concentrations from Meinshausen et al 2009[9] which include the effects of a number of GHGs. Red represents the SRES A1F1 scenario and blue the Meinshausen halved-by-2050 scenario.

Additional Methods: The model and experimental design for the ensemble are described in Stainforth et al. 2005[14]. The parameters perturbed in the experiment and the definitions of the regions analysed are presented in supplementary information 1.

The nature of the climate*prediction*.net project leads to a dataset which is unsurprisingly messy; some simulations do not complete, some do not return all of the data. Quality control procedures applied here were similar to those used in previous studies[14,30] . Before inclusion in this study each simulation was checked: i) for the existence of information on the parameter values used, ii) for the existence of files necessary to check the stability of the control phase and to calculate the regional data used herein, iii) to ensure that the drift in annual mean T_g in the last eight years of the control phase was no greater than 0.02 Kyr^{-1}, iv) to ensure the data was not corrupted, as

indicated by an inability to calculate a climate sensitivity[14] or jumps in seasonal means from one season to the next of more than 10K or 40mm/day, and v) to remove those showing unphysical cooling in the tropical east pacific using the method applied in Knight et al, 2007[30].

39802 simulations passed the data quality checks. Ensemble filtering involved the removal of half the model versions leaving 19618 simulations and 6203 model versions for inclusion here. Where duplicate simulations gave non-identical results, their mean was taken. Within each initial condition ensemble the regional and seasonal variance was calculated allowing for the impact of the deduced relationship on the uncertainty in the dependent variable.

While all simulations provided mean data for the last eight years of each phase, only 16378 of the 19618 simulations provided the regional timeseries data necessary for the calculation of time means from earlier in the phases for inclusion in figure 2. This extra data only became available for new runs following an upgrade to the distributed modelling software part way through the project.

Northern Europe was taken as 48N-75N, 10W-40E, and North Asia as 50N-70N 40E-180E, following Giorgi and Francisco, 2000[19], but including both land and sea points. Supplementary information contains information for other regions.

References

1. Stainforth, D. A., Allen, M. R., Tredger, E. R., and Smith, L. A., Confidence, uncertainty and decision-support relevance in climate predictions. Philosophical Transactions of the Royal Society a-Mathematical Physical and Engineering Sciences 365 (1857), 2145 (2007).

2. Tebaldi, C., Smith, R. L., Nychka, D., and Mearns, L. O., Quantifying uncertainty in projections of regional climate change: A Bayesian approach to the analysis of multimodel ensembles. Journal of Climate 18 (10), 1524 (2005).

3. Stott, P. A., Kettleborough, J. A., and Allen, M. R., Uncertainty in continental-scale temperature predictions. Geophysical Research Letters 33 (2) (2006).

4. Palmer, T. N. and Ralsanen, J., Quantifying the risk of extreme seasonal precipitation events in a changing climate. Nature 415 (6871), 512 (2002).

5. Raisanen, J. and Ruokolainen, L., Probabilistic forecasts of near-term climate change based on a resampling ensemble technique. Tellus Series a-Dynamic Meteorology and Oceanography 58 (4), 461 (2006).

6. Allen, M.R., Frame, D.J., Kettleborough, J., Stainforth, D.A. "Model error in weather and climate forecasting" in "Predictability of Weather and Climate". Cambridge University Press**,** ISBN-10: 0521848822**,** ISBN-13: 978-0521848824, pp 391-427 (2006).

7. Murphy, J.M. et al., UK Climate Projections Science Report: Climate change projections. Met Office Hadley Centre, Exeter. http://ukclimateprojections.defra.gov.uk (2009)

8. G8. Hokkaido Toyako Summit Leaders Declaration (G8, 2008); available at (www.mofa.go.jp/policy/economy/summit/2008/doc/doc080714__en.htm).

9. Meinshausen, M. et al., Greenhouse-gas emission targets for limiting global warming to 2 degrees C. Nature 458 (7242), 1158 (2009).

10. Hulme, M., Pielke, R., and Dessai, S. Keeping Prediction in perspective. Nature Reports Climate Change, 126 (2009)

11. Baker, M. B. and Roe, G. H., The Shape of Things to Come: Why Is Climate Change So Predictable? Journal of Climate 22 (17), 4574 (2009).

12. Frame, D. J. et al., Constraining climate forecasts: The role of prior assumptions. Geophysical Research Letters 32 (9) (2005).

13. Sokolov, A. P. et al., Probabilistic Forecast for Twenty-First-Century Climate Based on Uncertainties in Emissions (Without Policy) and Climate Parameters. Journal of Climate 22 (19), 5175 (2009).

14. Stainforth, D. A. et al., Uncertainty in predictions of the climate response to rising levels of greenhouse gases. Nature 433 (7024), 403 (2005)

15. Rodwell, M. J. and Palmer, T. N., Using numerical weather prediction to assess climate models. Quarterly Journal of the Royal Meteorological Society 133 (622), 129 (2007).

16. Joshi, M.M., Webb, M.J., Maycock, A.C., and Collins, M. Stratospheric water vapour and high climate sensitivity in a version of the HadSM3 climate model, Atmos. Chem. Phys. (2010).

17. Williams, K. D., Senior, C. A., and Mitchell, J. F. B., Transient climate change in the Hadley Centre models: The role of physical processes. Journal of Climate 14 (12), 2659 (2001).

18. Pope, V. D., Gallani, M. L., Rowntree, P. R., and Stratton, R. A., The impact of new physical parametrizations in the Hadley Centre climate model: HadAM3. Climate Dynamics 16 (2-3), 123 (2000).

19. Giorgi, F. & Francisco, R. Uncertainties in regional climate change prediction: a regional analysis of ensemble simulations with the HADCM2 coupled AOGCM. Climate Dynamics 16, 169-182 (2000)

20. Jun, M., Knutti, R., and Nychka, D. W., Spatial Analysis to Quantify Numerical Model Bias and Dependence: How Many Climate Models Are There? Journal of the American Statistical Association 103 (483), 934 (2008).

21. Abramowitz, G. and Gupta, H., Toward a model space and model independence metric. Geophysical Research Letters 35 (5) (2008).

22. Jun, M. Y., Knutti, R., and Nychka, D. W., Local eigenvalue analysis of CMIP3 climate model errors. Tellus Series a-Dynamic Meteorology and Oceanography 60 (5), 992 (2008).

23. Smith, L. A., What might we learn from climate forecasts? Proceedings of the National Academy of Sciences of the United States of America 99, 2487 (2002).

24. McWilliams, J. C., Irreducible imprecision in atmospheric and oceanic simulations. Proceedings of the National Academy of Sciences of the United States of America 104 (21), 8709 (2007).

25. Allen, M. R. and Ingram, W. J., Constraints on future changes in climate and the hydrologic cycle. Nature 419 (6903), 224 (2002).

26. Stainforth, D. A. et al., Issues in the interpretation of climate model ensembles to inform decisions. Philosophical Transactions of the Royal Society a-Mathematical Physical and Engineering Sciences 365 (1857), 2163 (2007).

27. Baldwin, M. P., Dameris, M., and Shepherd, T. G., Atmosphere - How will the stratosphere affect climate change? Science 316 (5831), 1576 (2007).

28. Notz, D., The future of ice sheets and sea ice: Between reversible retreat and unstoppable loss. Proceedings of the National Academy of Sciences of the United States of America 106 (49), 20590 (2009).

29. Friedlingstein, P. et al., Climate-carbon cycle feedback analysis: Results from the (CMIP)-M-4 model intercomparison. Journal of Climate 19 (14), 3337 (2006).

30. Knight, C.G. et al. Association of parameter, software, and hardware variation with large-scale behavior across 57,000 climate models. Proceedings of the

National Academy of Sciences of the United States of America 104, 12259-12264 (2007).

Table 1: Selected Regional, Seasonal Changes by the 2090s.

The predicted distribution of change in 8 year mean model climate by the 2090s for Northern Europe(NE) and North Asia (NA), temperature (T in Kelvin) and precipitation (Pr in %), and various seasons (Dec/Jan/Feb(DJF), Mar/Apr/May(MAM) etc.). The 5-95% range is presented for the A1F1 and the halved-by-2050 scenarios used in Meinshausen et al. 2009. Figures are only presented where the correlation coefficient with T_g is 0.8 or greater (see methods). This is an arbitrary cut-off which is useful simply in highlighting relationships of potential relevance. For NE and NA it identifies all relationships for which this approach has value.

Region	Session	Variable	Halved-by-2050		A1F1	
			5%	95%	5%	95%
NE	DJF	T	0.55	5.85	6.85	14.45
NE	MAM	T	0.15	4.65	5.05	11.65
NE	JJA	T	-0.05	4.25	3.45	9.45
NE	SON	T	0.15	4.15	4.05	9.95
NE	Annual	T	0.35	4.45	4.95	11.15
NA	DJF	T	0.25	6.35	6.35	15.25
NA	MAM	T	-0.25	4.85	3.75	10.95
NA	JJA	T	-0.95	4.75	1.75	9.35
NA	SON	T	0.35	4.65	4.75	11.45
NA	Annual	T	-0.05	4.75	4.25	11.35
NE	DJF	Pr	-5.5	33.5	22.5	70.5
NA	DJF	Pr	1.5	46.5	31.5	90.5
NA	MAM	Pr	-1.5	32.5	20.5	64.5
NA	SON	Pr	-0.5	25.5	16.5	49.5
NA	Annual	Pr	1.5	23.5	21.5	52.5

Figure 1:

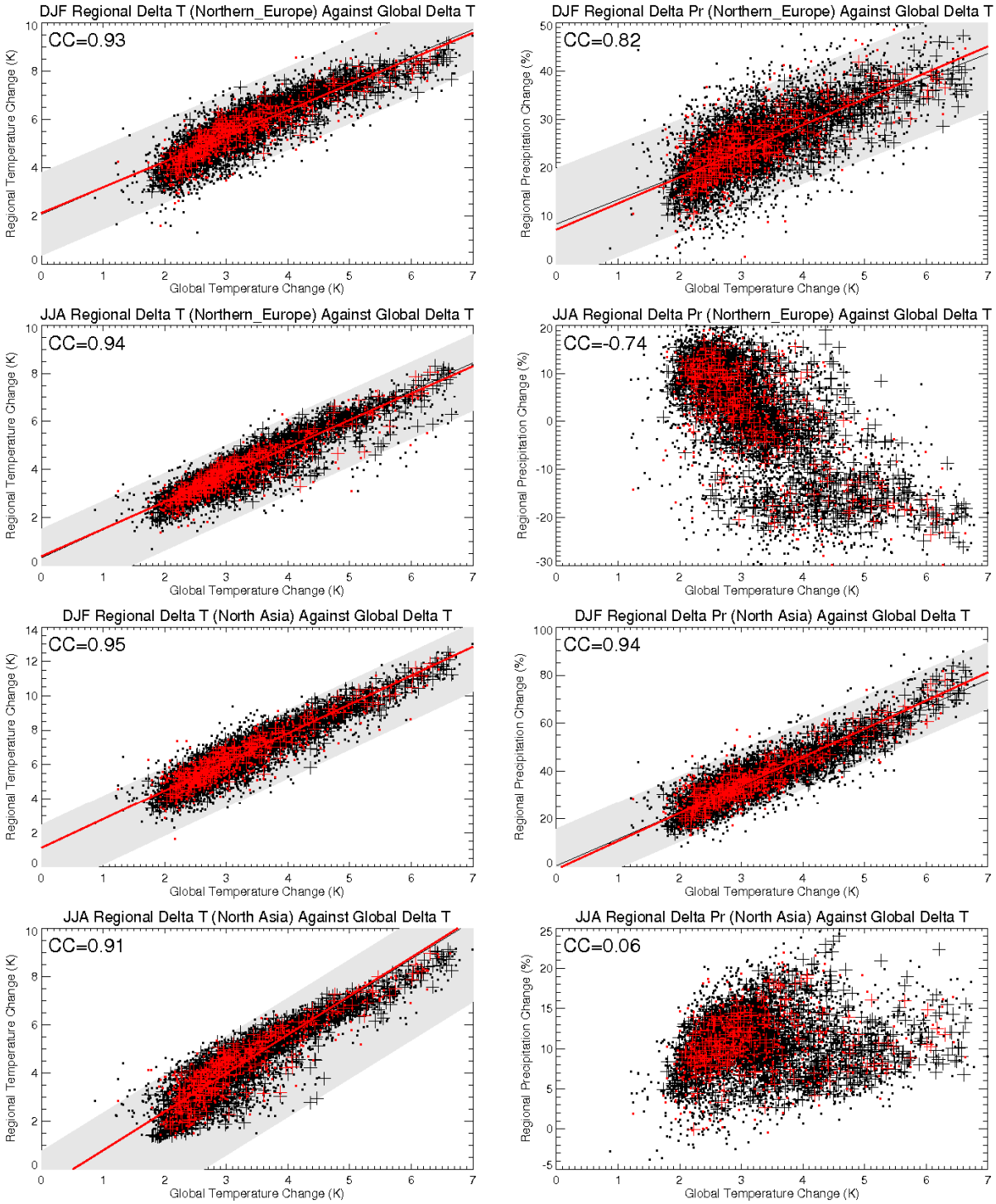
DJF Regional Delta T (Northern_Europe) Against Global Delta T
CC=0.93
DJF Regional Delta Pr (Northern_Europe) Against Global Delta T
CC=0.82
JJA Regional Delta T (Northern_Europe) Against Global Delta T
CC=0.94
JJA Regional Delta Pr (Northern_Europe) Against Global Delta T
CC=-0.74
DJF Regional Delta T (North Asia) Against Global Delta T
CC=0.95
DJF Regional Delta Pr (North Asia) Against Global Delta T
CC=0.94
JJA Regional Delta T (North Asia) Against Global Delta T
CC=0.91
JJA Regional Delta Pr (North Asia) Against Global Delta T
CC=0.06
Regional Temperature Change (K)
Regional Precipitation Change (%)
Global Temperature Change (K)

Figure 2:

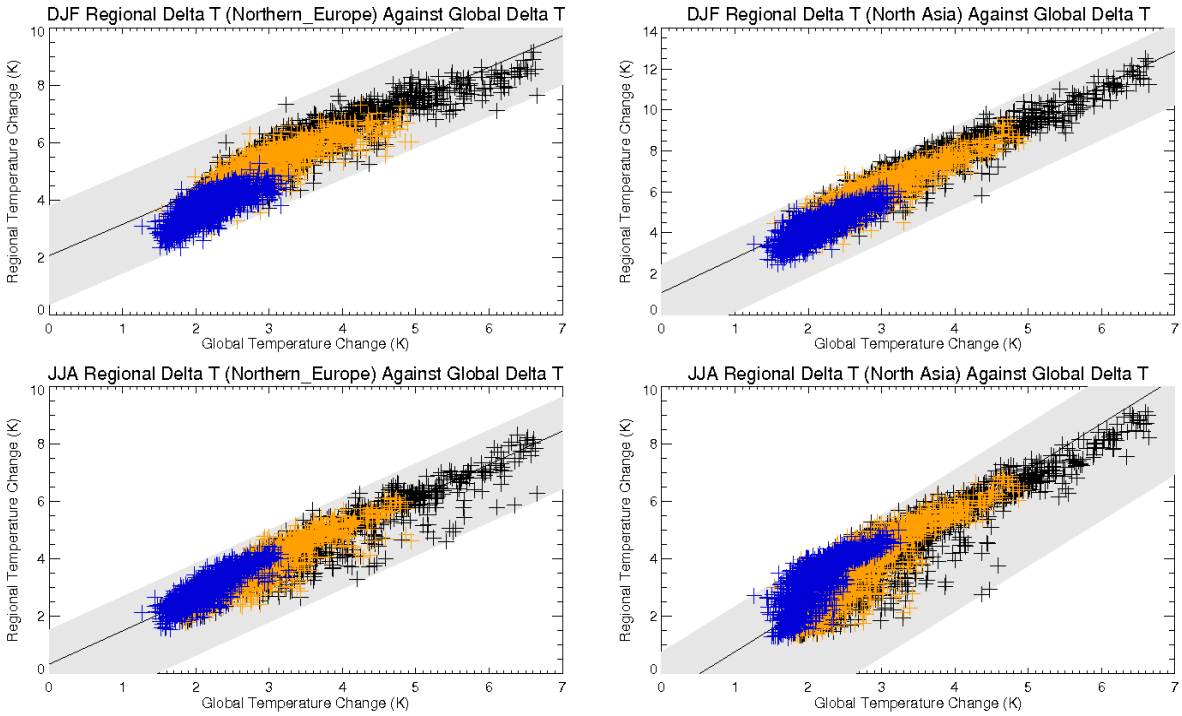
DJF Regional Delta T (Northern_Europe) Against Global Delta T
DJF Regional Delta T (North Asia) Against Global Delta T
JJA Regional Delta T (Northern_Europe) Against Global Delta T
JJA Regional Delta T (North Asia) Against Global Delta T
Regional Temperature Change (K)
Global Temperature Change (K)

Figure 3:

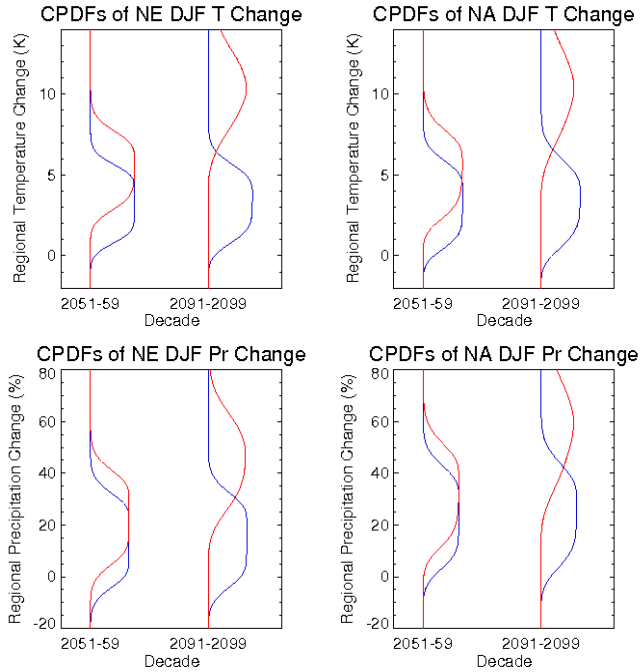
CPDFs of NE DJF T Change
CPDFs of NA DJF T Change
Regional Temperature Change (K)
10
5
0
2051-59
2091-2099
Decade
CPDFs of NE DJF Pr Change
CPDFs of NA DJF Pr Change
Regional Precipitation Change (%)
80
60
40
20
0
-20

Supplementary Information

Probabilistic Regional and Seasonal Predictions of Twenty-First Century Temperature and Precipitation

David A. Stainforth[1,2]

[1] *Grantham Research Institute, London School of Economics and Political Science, Houghton Street, London. WC2A 2AE*

[2] *Oxford University Centre for the Environment, University of Oxford, South Parks Road, Oxford. OX1 3QY*

Captions for Supplementary Figures

Supplementary Figure 1: As Figure 1 but for all regions and seasons. The shaded band is taken as having uniform probability. It is only plotted when the correlation coefficient is 0.8 or greater. This is an arbitrary cut off and in any case is only indicative of the potential usefulness of the correlation. A judgement of the relevance of the relationship should be made on a case by case basis but for plotting purposes it is useful to apply this criterion.

Supplementary Table 1: List of regions studied

The regions analysed were the same as those used in Giorgi and Francisco, 2000 but including both land and sea points. Their definitions are included here.

Name	**Latitude (°)**	**Longitude (°)**
Australia	45S-11S	110E-155E
Amazon Basin	20S-12N	82W-34W
Southern South America	56S-20S	76W-40W
Central America	10N-30N	116W-83W
Western North America	30N-60N	130W-103W
Central North America	30N-50N	103W-85W
Eastern North America	25N-50N	85W-60W
Alaska	60N-72N	170W-103W
Greenland	50N-85N	103W-10W
Mediterranean Basin	30N-48N	10W-40E
Northern Europe	48N-75N	10W-40E
Western Africa	12S-18N	20W-22E
Eastern Africa	12S-18N	22E-52E
Southern Africa	35S-12S	10W-52E
Sahara	18N-30N	20W-65E
Southeast Asia	11S-20N	95E-155E
East Asia	20N-50N	100E-145E
South Asia	5N-30N	65E-100E
Central Asia	30N-50N	40E-75E
Tibet	30N-50N	75E-100E
North Asia	50N-70N	40E-180E

Supplementary Table 2: Parameters Perturbed in the Ensemble

The parameters which were perturbed in the ensemble analysed herein.

Parameter	Component of GCM physics	Description/Process Affected
Vf1	Large scale cloud	Ice fall speed
Ct	Large scale cloud	Cloud droplet to rain conversion rate
Cw	Large scale cloud	Cloud droplet to rain conversion threshold
RHcrit	Large scale cloud	Threshold of relative humidity for cloud formation
EACF	Large scale cloud	Cloud fraction at saturation
EntCoef	Convection	Entrainment rate coefficient. Scales rate of mixing between environmental air and convective plume
Ice_size	Radiation	Effective radius of cloud ice spheres
Non-spherical ice particle parameters	Radiation	Parameters allowing for non-spherical ice particles in the radiation scheme
Alpham	Sea Ice	Albedo at melting point of ice
Dtice	Sea ice	The dependence of sea ice albedo on temperature

Supplementary Table 3: Parameter Values and Perturbation Codes

The identification code of each simulation included in this analysis is listed in supplementary table 5. Also listed is a "perturbation code" which identifies the model version of that simulation, i.e. the parameter perturbations which have been made. Each digit in the perturbation code represents the values of a different parameter or parameter group; "1" is always the standard value in the unperturbed model. The parameter values corresponding to each parameter code digit are given here.

		Value of this digit of the parameter code:				
		0	1	2	3	4
Parameter code digit	**Parameter**	**Corresponding Parameter values:**				
1st	alpham	-	0.5	0.57	0.65	
2nd	Ct	5e-5	1e-4	4e-4		
3rd	Cw_land CW_sea	1e-4 2e-5	2e-4 5e-5	2e-3 5e-4		
4th	dtice		10	5	2	<0
5th	EACF		0.5	0.7:0.6	0.8:0.65	
6th	entcoef	0.6	3.0	9.0		
7th	Non-spherical ice particle parameters: i_cnv_ice_lw i_cnv_ice_sw i_st_ice_sw i_st_ice_sw		 1 3 1 2	 7 7 7 7		
8th	ice_size	2.5e-5	3e-5	4e-5		
9th	rhcrit	0.6	0.7	0.9		
10th	vf1	0.5	1.0	2.0		

Supplementary Table 4: Regional, Seasonal Changes by 2090.

The predicted distribution of change in 8 year mean model climate by the 2090s for all regions and seasons in which the correlation coefficient with T_g is 0.8 or greater. The 5-95% range is presented for the A1F1 and the halved-by-2050 scenarios used in Meinshausen et al. 2009. Note: The 0.8 cut off is applied only as an indication of potential relevance of the relationship. The numbers in this table should be interpreted in the light of the judged relevance of the associated relationship in the plots in supplementary figure 1.

Region	Session	Variable	Halved-by-2050		A1F1	
			5%	95%	5%	95%
Australia	DJF	T	0.95	3.85	3.05	7.25
Australia	MAM	T	0.85	3.85	3.05	7.55
Australia	JJA	T	0.65	3.15	2.45	6.45
Australia	SON	T	1.05	4.05	3.35	7.75
Australia	Annual	T	1.05	3.65	3.15	7.25
Amazon_Basin	DJF	T	0.25	4.55	2.05	8.45
Amazon_Basin	MAM	T	0.65	4.95	2.85	9.25
Amazon_Basin	JJA	T	0.55	5.45	2.75	9.85
Amazon_Basin	SON	T	0.85	5.15	3.15	9.75
Amazon_Basin	Annual	T	0.75	4.95	2.85	9.25
Southern_South_America	DJF	T	0.25	2.75	1.65	5.75
Southern_South_America	MAM	T	-0.05	2.95	1.25	5.85
Southern_South_America	JJA	T	0.35	3.15	2.15	6.45
Southern_South_America	SON	T	0.25	2.95	1.95	6.25
Southern_South_America	Annual	T	0.35	2.85	1.85	5.95
Central_America	DJF	T	0.45	3.05	3.55	7.55
Central_America	MAM	T	0.95	3.65	3.95	8.35
Central_America	JJA	T	1.05	4.25	4.15	9.15
Central_America	SON	T	0.95	3.65	3.65	8.05

Central_America	Annual	T	1.05	3.45	3.95	8.15
Western_North_America	DJF	T	0.25	4.55	3.65	9.85
Western_North_America	MAM	T	0.05	3.65	3.55	8.75
Western_North_America	JJA	T	1.25	4.85	5.95	11.95
Western_North_America	SON	T	0.75	4.05	4.75	10.15
Western_North_America	Annual	T	0.95	4.05	4.75	10.05
Central_North_America	DJF	T	-0.35	5.95	5.25	13.25
Central_North_America	MAM	T	0.35	5.35	5.05	11.85
Central_North_America	JJA	T	0.85	6.95	6.55	15.05
Central_North_America	SON	T	0.15	5.65	4.45	12.05
Central_North_America	Annual	T	0.85	5.45	5.85	12.65
Eastern_North_America	DJF	T	0.35	4.65	5.15	11.25
Eastern_North_America	MAM	T	0.75	4.15	4.65	9.75
Eastern_North_America	JJA	T	1.05	4.05	5.15	10.15
Eastern_North_America	SON	T	1.05	4.05	4.95	9.85
Eastern_North_America	Annual	T	0.95	4.05	5.15	10.15
Alaska	DJF	T	0.05	9.65	6.45	18.55
Alaska	MAM	T	-0.35	5.15	4.45	11.95
Alaska	JJA	T	-0.65	3.65	1.55	7.25
Alaska	SON	T	0.55	5.75	6.85	14.45
Alaska	Annual	T	0.55	5.55	5.45	12.85
Alaska	MAM	Pr	-25.5	40.5	-19.5	54.5
Alaska	SON	Pr	-15.5	39.5	-1.5	61.5
Alaska	Annual	Pr	-12.5	32.5	2.5	56.5
Greenland	DJF	T	0.35	7.25	6.15	16.05
Greenland	MAM	T	0.35	5.05	4.65	11.15
Greenland	JJA	T	-0.25	3.15	2.35	7.15
Greenland	SON	T	0.05	4.75	4.75	11.45

Greenland	Annual	T	0.55	4.95	4.85	11.35
Greenland	DJF	Pr	-4.5	26.5	16.5	57.5
Greenland	MAM	Pr	-0.5	25.5	19.5	52.5
Greenland	SON	Pr	-2.5	24.5	19.5	53.5
Greenland	Annual	Pr	1.5	20.5	22.5	49.5
Mediterranean_Basin	DJF	T	0.85	4.15	4.85	9.95
Mediterranean_Basin	MAM	T	0.95	3.95	4.75	9.65
Mediterranean_Basin	JJA	T	1.15	5.45	5.65	12.35
Mediterranean_Basin	SON	T	1.05	4.25	4.65	9.95
Mediterranean_Basin	Annual	T	1.15	4.05	5.15	10.15
Northern_Europe	DJF	T	0.55	5.85	6.85	14.45
Northern_Europe	MAM	T	0.15	4.65	5.05	11.65
Northern_Europe	JJA	T	-0.05	4.25	3.45	9.45
Northern_Europe	SON	T	0.15	4.15	4.05	9.95
Northern_Europe	Annual	T	0.35	4.45	4.95	11.15
Northern_Europe	DJF	Pr	-5.5	33.5	22.5	70.5
Western_Africa	DJF	T	0.85	3.95	2.95	7.75
Western_Africa	MAM	T	1.05	4.15	3.25	8.05
Western_Africa	JJA	T	0.75	4.25	2.35	7.55
Western_Africa	SON	T	0.45	4.25	2.05	7.45
Western_Africa	Annual	T	0.85	4.15	2.75	7.65
Eastern_Africa	DJF	T	0.65	4.25	2.65	8.15
Eastern_Africa	MAM	T	0.85	4.55	3.25	8.95
Eastern_Africa	JJA	T	0.65	5.05	2.55	8.85
Eastern_Africa	SON	T	0.45	5.05	2.25	8.65
Eastern_Africa	Annual	T	0.85	4.65	2.75	8.55
Southern_Africa	DJF	T	0.85	3.15	2.65	6.45
Southern_Africa	MAM	T	0.95	3.35	3.05	6.95

Southern_Africa	JJA	T	0.85	3.25	2.55	6.55
Southern_Africa	SON	T	0.95	3.45	2.75	6.85
Southern_Africa	Annual	T	0.95	3.25	2.75	6.65
Sahara	DJF	T	0.75	3.85	3.85	8.85
Sahara	MAM	T	1.25	4.45	5.05	10.25
Sahara	JJA	T	1.35	5.35	5.55	11.55
Sahara	SON	T	1.25	4.75	4.95	10.55
Sahara	Annual	T	1.35	4.35	4.95	10.05
Southeast_Asia	DJF	T	0.65	3.15	2.85	6.65
Southeast_Asia	MAM	T	0.65	3.35	2.65	6.65
Southeast_Asia	JJA	T	0.75	3.45	2.65	6.75
Southeast_Asia	SON	T	0.75	3.55	2.95	6.95
Southeast_Asia	Annual	T	0.75	3.35	2.75	6.75
East_Asia	DJF	T	0.65	4.15	5.65	11.15
East_Asia	MAM	T	0.75	3.95	4.65	9.65
East_Asia	JJA	T	0.95	3.95	5.25	10.25
East_Asia	SON	T	0.95	3.65	4.95	9.65
East_Asia	Annual	T	0.95	3.85	5.15	10.05
South_Asia	DJF	T	0.75	4.45	4.05	9.25
South_Asia	MAM	T	0.95	4.15	3.75	8.55
South_Asia	JJA	T	0.45	4.65	2.45	7.75
South_Asia	SON	T	0.75	4.85	3.75	9.25
South_Asia	Annual	T	0.85	4.45	3.55	8.55
Central_Asia	DJF	T	-0.05	4.65	5.05	11.75
Central_Asia	MAM	T	0.45	5.35	5.55	12.45
Central_Asia	JJA	T	1.35	5.35	6.35	13.05
Central_Asia	SON	T	1.15	4.55	5.35	10.95
Central_Asia	Annual	T	1.45	4.75	6.25	11.95

Tibet	DJF	T	1.05	5.75	6.55	13.65
Tibet	MAM	T	1.05	5.25	5.45	11.75
Tibet	JJA	T	1.25	5.25	5.65	11.95
Tibet	SON	T	1.15	4.95	5.85	11.95
Tibet	Annual	T	1.45	4.95	6.05	12.05
Tibet	MAM	Pr	-15.5	31.5	-11.5	40.5
North_Asia	DJF	T	0.25	6.35	6.35	15.25
North_Asia	MAM	T	-0.25	4.85	3.75	10.95
North_Asia	JJA	T	-0.95	4.75	1.75	9.35
North_Asia	SON	T	0.35	4.65	4.75	11.45
North_Asia	Annual	T	-0.05	4.75	4.25	11.35
North_Asia	DJF	Pr	1.5	46.5	31.5	90.5
North_Asia	MAM	Pr	-1.5	32.5	20.5	64.5
North_Asia	SON	Pr	-0.5	25.5	16.5	49.5
North_Asia	Annual	Pr	1.5	23.5	21.5	52.5
Antarctica	DJF	T	-0.25	2.85	0.75	4.85
Antarctica	MAM	T	-0.35	5.15	1.75	8.85
Antarctica	JJA	T	0.15	5.95	3.05	10.85
Antarctica	SON	T	0.25	4.25	2.65	8.15
Antarctica	Annual	T	0.35	4.35	2.35	8.05
Antarctica	DJF	Pr	-1.5	26.5	3.5	41.5
Antarctica	MAM	Pr	1.5	28.5	5.5	45.5
Antarctica	JJA	Pr	-0.5	35.5	12.5	62.5
Antarctica	SON	Pr	-5.5	28.5	0.5	44.5
Antarctica	Annual	Pr	0.5	27.5	6.5	47.5

Supplementary Table 5: List of simulations and perturbations

The run ids for all simulations are listed along with the perturbation code identifying how parameters have been perturbed. This table can be found in supplementary_information_table_5_simulations.xls